LANDAU WEEK 2023

115 year jubilee

TWO-DIMENSIONAL HIGHER-ORDER TOPOLOGICAL SUPERCONDUCTOR WITH ELECTRON-ELECTRON INTERACTIONS

Sergey Aksenov, Sasha Fedoseev, Maxim Shustin, Anton Zlotnikov

Kirensky Institute of Physics, Federal Research Center KSC SB RAS, Krasnoyarsk, Russia

email: asv86@iph.krasn.ru

Abstract

Here we present the results of an analytical and numerical study of the Coulomb interaction problem in one of the standard models of a higher-order topological superconductor (HOTSC) [1,2]. The attention is paid to both limiting cases: weak and strong charge correlations [3]. In the first situation, it is shown that the boundaries of the topologically nontrivial phase are extended due to the many-body interaction. For a system with open boundary conditions, a crossover of the ground state was found. If the repulsion intensity is lower than the critical, the charge density distribution has C_4 symmetry and does not depend on spin, and the energy of the Majorana corner state is determined by the overlap of the wave functions localized in different corners. After the crossover, the concentration correlator depends on the spin projection and has a spontaneously broken symmetry. In turn, the energy of the corner state ceases to depend on the system size. The dependence of this crossover on the shape of the boundary of the 2D system is discussed. The possibility to realize the Majorana corner states in the limit of the infinitely strong repulsion is demonstrated based on the analysis of the Dirac mass of edge Hubbard fermions. It is shown that the boundaries of the topologically nontrivial phase become strongly renormalized due to the Hubbard corrections.

Model of HOTSC with Electron Correlations

Recently, the minimal model of HOTSC describing a 2D topological insulator (transition-metal dichalcogenides and rocksalt IV-VI semiconductors XY (X = Ge, Sn, Pb and Y = S, Se, Te) [4, 5]) proximitized by an $s_{\pm}$-wave superconductor was proposed [1].

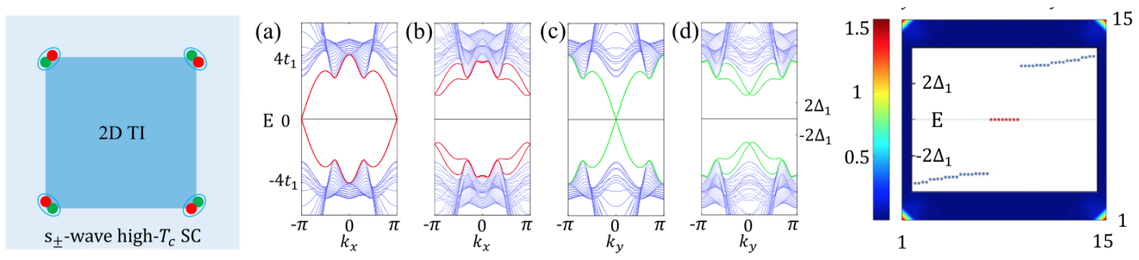

Figure 1: Left: Schematics of HOTSC. Middle: Band structure of a 2D ribbon of topological insulator with [(b), (d)] and without [(a), (c)] superconductivity. Right: The energy spectrum and density plot for a 2D lattice. The results and figures from [1].

The model of HOTSC with Hubbard repulsion.

$$
\begin{aligned}
H \;=\; & \sum_{f\eta\sigma} (\eta\Delta\varepsilon - \mu)\, c^{+}_{f\eta\sigma} c_{f\eta\sigma} + \sum_{\eta} \eta \left(\sum_{\langle fm\rangle_x,\sigma} t_x + \sum_{\langle fm\rangle_y,\sigma} t_y + \sum_{\langle\langle fm\rangle\rangle,\sigma} t_1 \right) c^{+}_{f\eta\sigma} c_{m\eta\sigma} + i\alpha \sum_{\langle fm\rangle} \left[\hat{\tau}^{\alpha\beta}, \boldsymbol{e}_{fm}\right]_z \hat{\sigma}^{\nu\eta}_x c^{+}_{f\nu\alpha} c_{m\eta\beta} \\
& + \left\{ \left(\Delta_x \sum_{\langle fm\rangle_x,\eta} + \Delta_y \sum_{\langle fm\rangle_y,\eta} \right) c^{+}_{f\eta\uparrow}\, c^{+}_{m\eta\downarrow} + \Delta_0 \sum_{f\eta} c^{+}_{f\eta\uparrow}\, c^{+}_{f\eta\downarrow} \right\} + \{h.c.\} + \sum_{f\eta} U_\eta n_{f\eta\uparrow}\, n_{f\eta\downarrow}, \qquad (1)
\end{aligned}
$$

where $c_{fA(B)\sigma}$ annihilates an electron with a spin σ on an Ath (Bth) orbital at the square lattice site f. An on-site energy shift $\Delta\varepsilon$ relative to a chemical potential μ has opposite sign for the different orbitals. The intraorbital nearest-neighbor $t_{x,y}$ hopping parameter has the same property and $t_x = -t_y$. The parameter α defines an intensity of the interorbital Rashba spin-orbit coupling. The parameters $\Delta_{0,1}$ are intensities of the intraorbital on-site and intersite singlet pairing that results in overall $s_{\pm}$-superconductivity. U is a strength of the intraorbital Coulomb interaction.
Mean-field approximation for the two-orbital HOTSC Hamiltonian:

$$
H_U \approx U \sum_{f\eta\sigma} \left[\langle n_{f\eta\sigma}\rangle n_{f\eta\bar{\sigma}} - \langle c^{+}_{f\eta\sigma} c_{f\eta\bar{\sigma}}\rangle c^{+}_{f\eta\bar{\sigma}} c_{f\eta\sigma} \right] - U \sum_{f\eta} \left[\langle c^{+}_{f\eta\uparrow}\; c^{+}_{f\eta\downarrow}\rangle c_{f\eta\uparrow}\; c_{f\eta\downarrow} - \langle c_{f\eta\uparrow}\; c_{f\eta\downarrow}\rangle c^{+}_{f\eta\uparrow}\; c^{+}_{f\eta\downarrow} \right]. \qquad (2)
$$

The ground-state energy for the different solutions for correlators:

$$
E_{gr} = -\sum_{f\eta n\sigma} |v_{f\eta n\sigma}|^2 \varepsilon_n - U \sum_{f\eta\sigma} \left[\langle n_{f\eta\uparrow}\;\rangle\langle n_{f\eta\downarrow}\rangle + |\langle c^{+}_{f\eta\uparrow}\; c^{+}_{f\eta\downarrow}\rangle|^2 \right]. \qquad (3)
$$

Crossover of the ground state in the weak-interaction regime. Spontaneously broken C_4 symmetry and nonzero magnetization near the corners

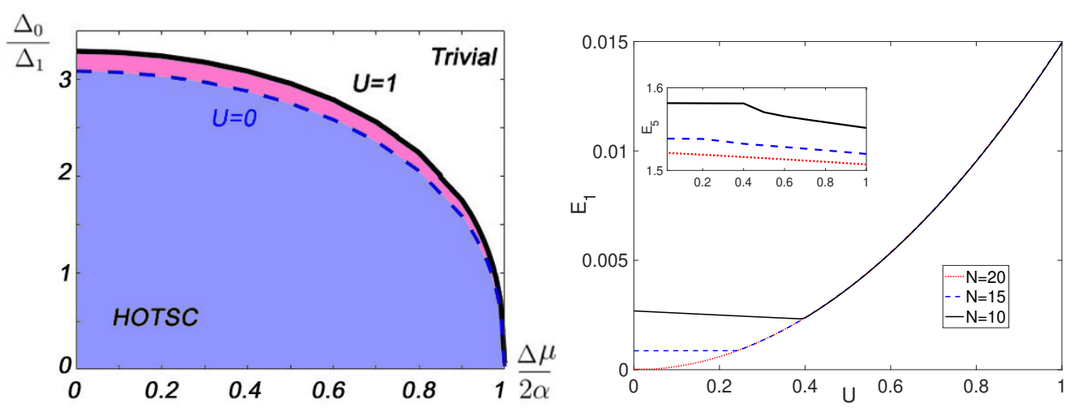

Figure 2: Left: Topological phase diagram of the 2D square-shaped topological insulator with extended s-wave superconducting coupling without Coulomb interaction $U = 0$ (blue region with blue dashed-line border) and with on-site Coulomb interaction $U = 1$ (blue and red region with black solid-line border). $\mu = \mu\mu_{hf}$ is chemical potential measured from the half-filling level. Right: Dependence of the first excitation energy on the intensity of the intraorbital Hubbard repulsion, $E_1(U)$, for different sizes of the square-shaped system. Inset: the energy of the first out-of-gap state as a function of U. The system is taken at half filling ($\mu_{hf} = U/2$). The other parameters are $\Delta_0 = \Delta\varepsilon = 0$, $t_x = -t_y = 2$, $t_1 = t_x/2$, $\Delta_1 = 0.5$, $\alpha = 1.5$ [3].

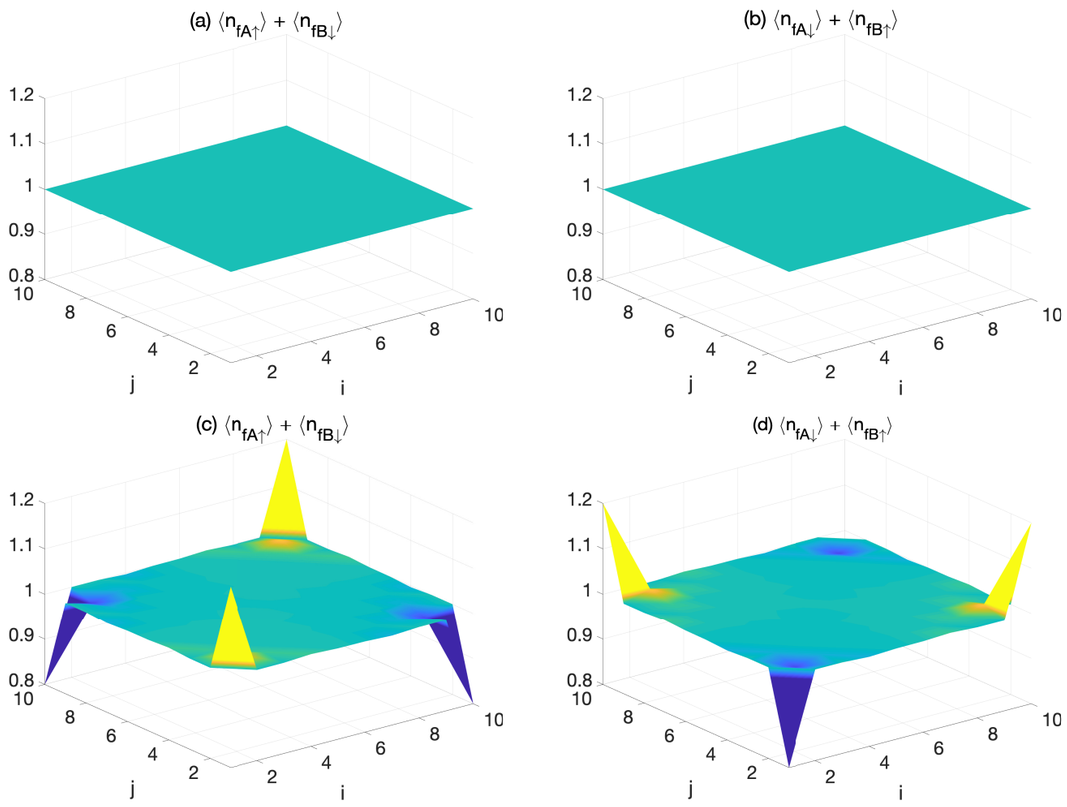

Figure 3: Spatial distribution of the correlators $\langle n_{fA\uparrow}\;\rangle + \langle n_{fB\downarrow}\rangle$ and $\langle n_{fA\downarrow}\rangle + \langle n_{fB\uparrow}\;\rangle$ (electron occupancies in the ground state) in the C_4-symmetric phase (a,b) and in the phase with the spontaneously broken C_4 symmetry (c,d).

Effect of boundary shape. Triangle

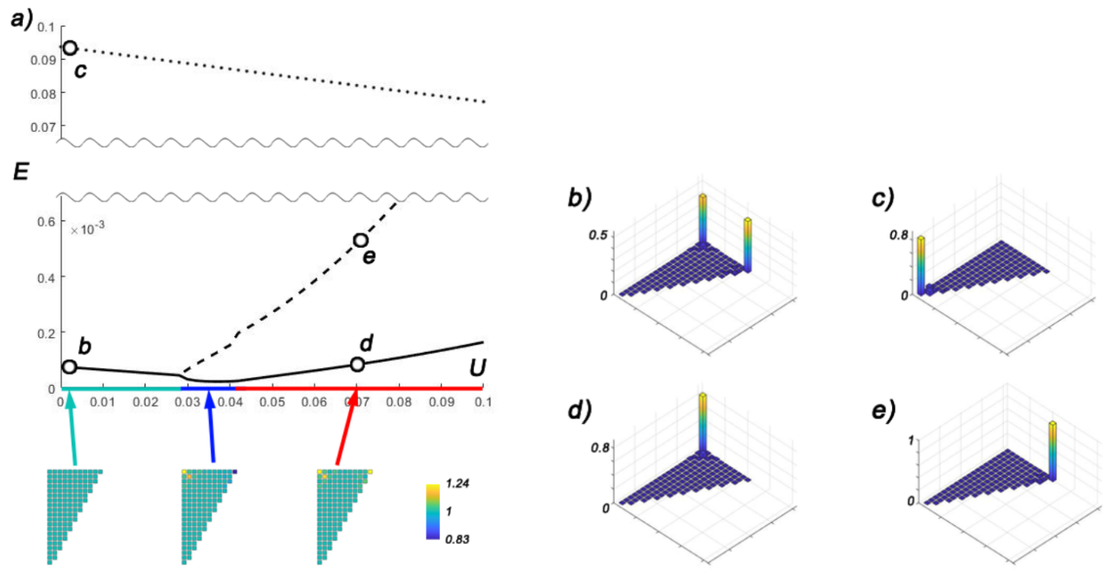

Figure 4: Left: Spectrum and $n_{A\downarrow} + n_{B\uparrow}$ quantity in the HOTSC with triangle-shaped 20×11 geometry. The system experience two transitions $fs \to (0+-) \to (0++)$ with deviations of $n_{A\downarrow} + n_{B\uparrow}$ appearing only at the corners, at which topological corner excitations present. Right: b-e) The corner excitations spatial distribution at corresponding points on a) [3].

$U \to \infty$ limit. Topological phase diagram and Dirac mass criterion

In the limit $U \to \infty$ Hamiltonian $\mathcal{H}_{eff}$ is reduced to

$$
\begin{aligned}
\mathcal{H}_{U\to\infty} \;=\; & P\mathcal{H}P = \sum_{f\sigma} \sum_{\eta=A,B} (-\mu + l_\eta \Delta\varepsilon)\, X^{\sigma\sigma}_{f\eta} + \sum_{f\eta\sigma} \sum_{\delta=x,y} t_\delta l_\eta \left(X^{\sigma 0}_{f\eta} X^{0\sigma}_{f+\delta,\eta} + h.c. \right) + \sum_{f\delta\eta\sigma} \left(\alpha_{\sigma\delta} X^{\sigma 0}_{f\eta} X^{0\bar{\sigma}}_{f+\delta,\bar{\eta}} + h.c. \right) \\
& + \sum_{f\eta} \sum_{\delta=\pm x,\pm y} \left(\Delta_1 X^{\uparrow\;0}_{f\eta} X^{\downarrow 0}_{f+\delta,\eta} + h.c. \right), \qquad (4)
\end{aligned}
$$

where $l_A = +1$, $l_B = -1$, $t_x = -t_y = t$, $\alpha_{\sigma x} = \alpha\sigma$, $\alpha_{\sigma y} = -i\alpha$.
The equation of motion for the operator $X^{0\sigma}_{f\eta}(t)$ in the Heisenberg representation and for the Hamiltonian (4) is expressed in the Hubbard-I approximation as

$$
i\frac{d}{dt} X^{0\sigma}_{f\eta} = (-\mu + \eta\Delta\varepsilon)\, X^{0\sigma}_{f\eta} + \sum_{\delta=\pm x,\pm y} t_\delta \eta H_{f\eta\sigma} X^{0\sigma}_{f+\delta\eta} + \sum_{\delta} \alpha_{\sigma\delta} H_{f\eta\sigma} X^{0\bar{\sigma}}_{f+\delta,\bar{\eta}} + \sum_{\delta} \Delta_1 \sigma H_{f\eta\sigma} X^{\bar{\sigma}0}_{f+\delta,\eta}, \qquad (5)
$$

where the Hubbard renormalization parameter is $H_{f\eta\sigma} = 1 - \left\langle X^{\bar{\sigma}\bar{\sigma}}_{f\eta} \right\rangle$. As in the case $U = 0$ spin-flip correlators $\left\langle X^{\bar{\sigma}0}_{f\eta} X^{0\sigma}_{f\eta} \right\rangle$ are neglected. We use the Zubarev's Green functions. In the uniform case $H_{f\eta\sigma} \equiv H_\eta = 1 - n_\eta/2$ and $n_\eta = \sum_\sigma \left\langle X^{\sigma\sigma}_{f\eta} \right\rangle$. The effective Hamiltonian in the Hubbard-I approximation can be pulled out of the equations of motion for the Green's functions, since, in general, $\hat{H}_{eff} = \omega \cdot \hat{I} - \hat{G}^{-1}$. The wave functions of the edge states along x- and y-directions were obtained for the continuum limit by expanding the effective Hamiltonian around the Dirac point $(k_{x0}, k_{y0}) = (0, \pi)$ or $(\pi, 0)$. As a result, the Dirac mass ratio is

$$
\frac{M_{D_x}}{M_{D_y}} = \frac{2(c_x + c_y) - c_x p_0^2 - c_y |\kappa_y|^2}{2(c_x + c_y) - c_x |\kappa_x|^2 - c_y p_0^2} = -1, \qquad (6)
$$

$$
|\kappa_x|^2 = |\kappa_y|^2 = \sqrt{\frac{t_A t_B p_0^4 + [c_x \tau_{AB} + \alpha_A \alpha_B]\, p_0^2 - m_A m_B}{t_A t_B}},
$$

$$
p_0^2 = \frac{[\mu (H_A + H_B) + \Delta\varepsilon (H_A - H_B)]^2}{16 H_A^2 H_B^2 \alpha^2}, \qquad (7)
$$

where $c_{x,y} \equiv \cos k_{x0,y0}$; $m_l = -\mu + \eta\Delta\varepsilon + 2\eta t_l (c_x - c_y)$; $\tau_{AB} = t_A m_B - t_B m_A$; $t_l = t H_l$, $\alpha_l = 2\alpha H_l$ (as usual $\eta = \pm 1$ if $l = A, B$). The wave vector p_0 is a new Dirac point shifted from (k_{x0}, k_{y0}) due to the strong many-body interactions.

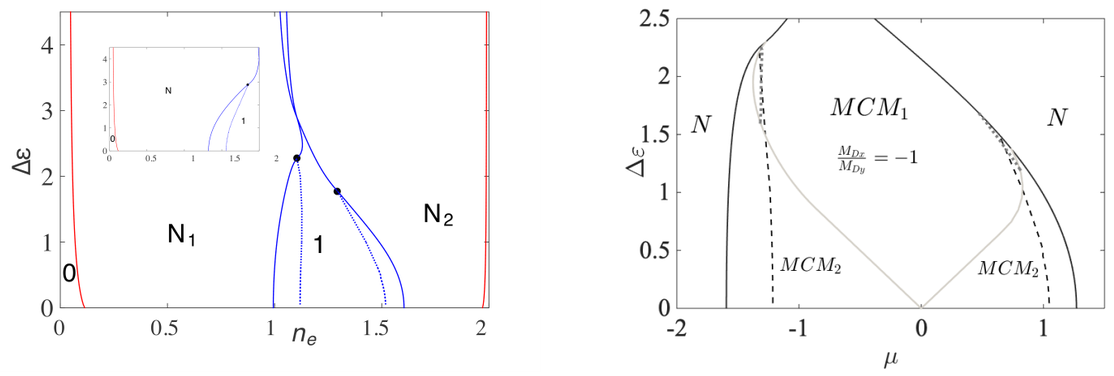

Figure 5: Left: Phase diagram of HOTSC at $U \to \infty$ in the variables n_e (electron concentration per site), $\Delta\varepsilon$ (orbital splitting). N is nodal phase, 1 is topological phase with Majorana corner modes. At solid lines the bulk spectrum of HOTSC is gapless, at dashed lines the spectrum of the ribbon with (01) or (10) edges is gapless. The parameters are $\alpha = 3/4t$, $\Delta_0 = 0$, $\Delta_1 = 0.5t$. Inset: case $U = 0$. Right: Parameter area of existence of Majorana corner modes. [3].

References

1. Q. Wang, C.-C. Liu, Y.-M. Lu and F. Zhang, Phys. Rev. Lett. 121, 186801 (2018).
2. A. O. Zlotnikov, M. S. Shustin, and A. D. Fedoseev, J Supercond Nov Magn 34, 3053 (2021).
3. S. V. Aksenov, A. D. Fedoseev, M. S. Shustin, and A. O. Zlotnikov, Phys. Rev. B 107, 125401 (2023).
4. Z. Wang, B. J. Wieder, J. Li, B. Yan, and B. A. Bernevig, Phys. Rev. Lett. 123, 186401 (2019).
5. J. W. Liu, X. F. Qian, and L. Fu, Nano Lett. 15, 2657 (2015).

The study was supported by Russian Science Foundation, project 22-22-20076, and Krasnoyarsk Regional Fund of Science.